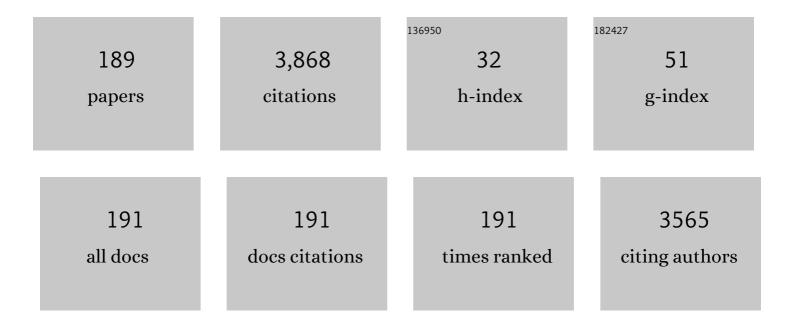
Florinda Costa

List of Publications by Year in descending order

Source: https://exaly.com/author-pdf/1787040/publications.pdf Version: 2024-02-01



#	Article	IF	CITATIONS
1	Laserâ€Induced Graphene Strain Sensors Produced by Ultraviolet Irradiation of Polyimide. Advanced Functional Materials, 2018, 28, 1805271.	14.9	228
2	Molecularly-imprinted chloramphenicol sensor with laser-induced graphene electrodes. Biosensors and Bioelectronics, 2019, 124-125, 167-175.	10.1	135
3	Synthesis of Long ZnO Nanorods under Microwave Irradiation or Conventional Heating. Journal of Physical Chemistry C, 2014, 118, 14629-14639.	3.1	120
4	Laser-Induced Graphene from Paper for Mechanical Sensing. ACS Applied Materials & Interfaces, 2021, 13, 10210-10221.	8.0	115
5	Effect of solvents on ZnO nanostructures synthesized by solvothermal method assisted by microwave radiation: a photocatalytic study. Journal of Materials Science, 2015, 50, 5777-5787.	3.7	105
6	Immunosensing Based on Optical Fiber Technology: Recent Advances. Biosensors, 2021, 11, 305.	4.7	83
7	Cortisol AuPd plasmonic unclad POF biosensor. Biotechnology Reports (Amsterdam, Netherlands), 2021, 29, e00587.	4.4	76
8	Biocompatibility evaluation of DLC-coated Si3N4 substrates for biomedical applications. Diamond and Related Materials, 2008, 17, 878-881.	3.9	73
9	Preparation of high-performance Ca3Co4O9 thermoelectric ceramics produced by a new two-step method. Journal of the European Ceramic Society, 2013, 33, 1747-1754.	5.7	73
10	Label-free plasmonic immunosensor for cortisol detection in a D-shaped optical fiber. Biomedical Optics Express, 2022, 13, 3259.	2.9	73
11	Sintered NbO Powders for Electronic Device Applications. Journal of Physical Chemistry C, 2011, 115, 4879-4886.	3.1	61
12	Effect of processing method on physical properties of Nb2O5. Journal of the European Ceramic Society, 2011, 31, 501-506.	5.7	61
13	A Review on the Applications of Graphene in Mechanical Transduction. Advanced Materials, 2022, 34, e2101326.	21.0	59
14	Microwave plasma chemical vapour deposition diamond nucleation on ferrous substrates with Ti and Cr interlayers. Diamond and Related Materials, 2002, 11, 1617-1622.	3.9	58
15	IR and UV Laserâ€Induced Graphene: Application as Dopamine Electrochemical Sensors. Advanced Materials Technologies, 2021, 6, 2100007.	5.8	58
16	New method to improve the grain alignment and performance of thermoelectric ceramics. Materials Letters, 2012, 83, 144-147.	2.6	53
17	Laserâ€Induced Graphene Piezoresistive Sensors Synthesized Directly on Cork Insoles for Gait Analysis. Advanced Materials Technologies, 2020, 5, 2000630.	5.8	53
18	Very Large Superconducting Currents Induced by Growth Tailoring. Crystal Growth and Design, 2015, 15, 2094-2101	3.0	52

2

Florinda Costa

#	Article	IF	CITATIONS
19	Adhesion behaviour assessment on diamond coated silicon nitride by acoustic emission. Diamond and Related Materials, 2003, 12, 733-737.	3.9	50
20	Cortisol in-fiber ultrasensitive plasmonic immunosensing. IEEE Sensors Journal, 2020, , 1-1.	4.7	49
21	YSZ:Dy3+ single crystal white emitter. Journal of Materials Chemistry, 2011, 21, 15262.	6.7	45
22	A critical review on the production and application of graphene and graphene-based materials in anti-corrosion coatings. Critical Reviews in Solid State and Materials Sciences, 2022, 47, 309-355.	12.3	45
23	Effect of N2 and H2 plasma treatments on band edge emission of ZnO microrods. Scientific Reports, 2015, 5, 10783.	3.3	43
24	A new interlayer approach for CVD diamond coating of steel substrates. Diamond and Related Materials, 2004, 13, 828-833.	3.9	42
25	CVD micro/nanocrystalline diamond (MCD/NCD) bilayer coated odontological drill bits. Diamond and Related Materials, 2009, 18, 264-270.	3.9	41
26	Wear resistant CVD diamond tools for turning of sintered hardmetals. Diamond and Related Materials, 2003, 12, 738-743.	3.9	39
27	Laserâ€Induced Graphene from Paper by Ultraviolet Irradiation: Humidity and Temperature Sensors. Advanced Materials Technologies, 2022, 7, .	5.8	39
28	Structural and optical properties of europium doped zirconia single crystals fibers grown by laser floating zone. Journal of Applied Physics, 2011, 109, .	2.5	38
29	Tailoring Ca3Co4O9 microstructure and performances using a transient liquid phase sintering additive. Journal of the European Ceramic Society, 2016, 36, 1025-1032.	5.7	38
30	Red light from ZrO2:Eu3+ nanostructures. Materials Science and Engineering B: Solid-State Materials for Advanced Technology, 2012, 177, 712-716.	3.5	36
31	Textured Bi–Sr–Ca–Cu–O rods processed by laser floating zone from solid state or melted precursors. Physica C: Superconductivity and Its Applications, 2004, 415, 163-171.	1.2	35
32	Phase transformation kinetics during thermal annealing of LFZ Bi–Sr–Ca–Cu–O superconducting fibers in the range 800–870°C. Physica C: Superconductivity and Its Applications, 1999, 323, 23-41.	1.2	34
33	Tribological behaviour of CVD diamond films on steel substrates. Wear, 2003, 255, 846-853.	3.1	34
34	Hot-filament chemical vapour deposition of nanodiamond on silicon nitride substrates. Diamond and Related Materials, 2004, 13, 643-647.	3.9	32
35	Laser-induced graphene from paper for non-enzymatic uric acid electrochemical sensing in urine. Carbon, 2022, 197, 253-263.	10.3	32
36	Optical and dielectric behaviour of EuNbO4 crystals. Journal of Materials Chemistry C, 2013, 1, 2913.	5.5	30

#	Article	IF	CITATIONS
37	Nano- and micro-crystalline diamond growth by MPCVD in extremely poor hydrogen uniform plasmas. Diamond and Related Materials, 2007, 16, 757-761.	3.9	29
38	Use of laser technology to produce high thermoelectric performances in Bi2Sr2Co1.8Ox. Materials & Design, 2015, 75, 143-148.	5.1	29
39	Optical properties of LFZ grown β-Ga2O3:Eu3+ fibres. Applied Surface Science, 2012, 258, 9157-9161.	6.1	28
40	Mechanical properties evaluation of fluor-doped diamond-like carbon coatings by nanoindentation. Thin Solid Films, 2004, 446, 85-90.	1.8	27
41	Colossal dielectric constant of poly- and single-crystalline CaCu3Ti4O12 fibres grown by the laser floating zone technique. Acta Materialia, 2011, 59, 102-111.	7.9	27
42	Effect of Current Polarity on BSCCO/Ag Ceramics Textured by Electrically Assisted Laser Floating Zone. Journal of Superconductivity and Novel Magnetism, 2013, 26, 943-946.	1.8	26
43	High thermoelectric performance in Bi2-xPbxBa2Co2Oy promoted by directional growth and annealing. Journal of the European Ceramic Society, 2016, 36, 67-74.	5.7	26
44	Wettability studies of reactive brazing alloys on CVD diamond plates. Diamond and Related Materials, 2001, 10, 775-780.	3.9	25
45	Thermal conductivity enhancement in cutting tools by chemical vapor deposition diamond coating. Diamond and Related Materials, 2002, 11, 703-707.	3.9	25
46	Mechanical behaviour of zirconia–mullite directionally solidified eutectics. Materials & Design, 2014, 61, 211-216.	5.1	25
47	Effects of Mn doping on the electrical and dielectric properties of CaCu 3 Ti 4 O 12 fibres. Ceramics International, 2014, 40, 16503-16511.	4.8	25
48	A mixture toxicity approach to predict the toxicity of Ag decorated ZnO nanomaterials. Science of the Total Environment, 2017, 579, 337-344.	8.0	25
49	Electrical field freezing effect on laser floating zone (LFZ)-grown Bi2Sr2Ca2Cu4O11superconducting fibres. Superconductor Science and Technology, 2004, 17, 612-619.	3.5	24
50	Bright room-temperature green luminescence from YSZ:Tb3+. Materials Letters, 2011, 65, 1979-1981.	2.6	24
51	ZnO nanostructures grown on vertically aligned carbon nanotubes by laser-assisted flow deposition. Acta Materialia, 2012, 60, 5143-5150.	7.9	24
52	Diffusion phenomena and crystallization path during the growth of LFZ Bi-Sr-Ca-Cu-O superconducting fibres. Superconductor Science and Technology, 2001, 14, 910-920.	3.5	23
53	One-step synthesis of ZnO decorated CNT buckypaper composites and their optical and electrical properties. Materials Science and Engineering B: Solid-State Materials for Advanced Technology, 2015, 195, 38-44.	3.5	23
54	ZnO decorated laser-induced graphene produced by direct laser scribing. Nanoscale Advances, 2019, 1, 3252-3268.	4.6	23

#	Article	IF	CITATIONS
55	A review on the laser-assisted flow deposition method: growth of ZnO micro and nanostructures. CrystEngComm, 2019, 21, 1071-1090.	2.6	23
56	Tunable green to red ZrO ₂ :Er nanophosphors. RSC Advances, 2015, 5, 20138-20147.	3.6	22
57	Effect of microwave power and nitrogen addition on the formation of {100} faceted diamond from microcrystalline to nanocrystalline. Vacuum, 2011, 85, 1130-1134.	3.5	21
58	Influence of SiC particle addition on the nucleation density and adhesion strength of MPCVD diamond coatings on Si 3 N 4 substrates. Diamond and Related Materials, 2000, 9, 483-488.	3.9	20
59	MPCVD diamond tool cutting-edge coverage: dependence on the side wedge angle. Diamond and Related Materials, 2001, 10, 803-808.	3.9	20
60	Surface Pretreatments of Silicon Nitride for CVD Diamond Deposition. Journal of the American Ceramic Society, 2003, 86, 749-754.	3.8	20
61	Tailored Si3N4Ceramic Substrates for CVD Diamond Coating. Surface Engineering, 2003, 19, 410-416.	2.2	20
62	Single and polycrystalline mullite fibres grown by laser floating zone technique. Journal of the European Ceramic Society, 2010, 30, 3311-3318.	5.7	20
63	Conversion of paper and xylan into laser-induced graphene for environmentally friendly sensors. Diamond and Related Materials, 2022, 123, 108855.	3.9	20
64	Luminescence studies on SnO2 and SnO2:Eu nanocrystals grown by laser assisted flow deposition. Physical Chemistry Chemical Physics, 2015, 17, 13512-13519.	2.8	19
65	Simultaneous CVD synthesis of graphene-diamond hybrid films. Carbon, 2016, 98, 99-105.	10.3	19
66	Exploring the potential of laser assisted flow deposition grown ZnO for photovoltaic applications. Materials Chemistry and Physics, 2016, 177, 322-329.	4.0	18
67	Diamond-Graphite Nanoplatelet Surfaces as Conductive Substrates for the Electrical Stimulation of Cell Functions. ACS Applied Materials & amp; Interfaces, 2017, 9, 1331-1342.	8.0	18
68	Directionally solidified eutectic and off-eutectic mullite–zirconia fibres. Journal of the European Ceramic Society, 2013, 33, 953-963.	5.7	17
69	Upconversion luminescence and blackbody radiation in tetragonal YSZ co-doped with Tm ³⁺ and Yb ³⁺ . Nanoscale, 2015, 7, 19958-19969.	5.6	17
70	Electrochemical Response of Glucose Oxidase Adsorbed on Laser-Induced Graphene. Nanomaterials, 2021, 11, 1893.	4.1	17
71	Title is missing!. Journal of Materials Science: Materials in Electronics, 2001, 12, 269-271.	2.2	16
72	Unstressed PACVD diamond films on steel pre-coated with a composite multilayer. Surface and Coatings Technology, 2005, 191, 102-107.	4.8	16

#	Article	IF	CITATIONS
73	Enhancement of superconductivity in LFZ-grown BSCCO fibres by steeper axial temperature gradients. Applied Surface Science, 2012, 258, 9175-9180.	6.1	16
74	Physical Structure and Electrochemical Response of Diamond–Graphite Nanoplatelets: From CVD Synthesis to Label-Free Biosensors. ACS Applied Materials & Interfaces, 2019, 11, 8470-8482.	8.0	16
75	The role of surface activation prior to seeding on CVD diamond adhesion. Surface and Coatings Technology, 2010, 204, 3585-3591.	4.8	15
76	Tuning the field emission of graphene-diamond hybrids by pulsed methane flow CVD. Carbon, 2017, 122, 726-736.	10.3	15
77	Radial inhomogeneities induced by fiber diameter in electrically assisted LFZ growth of Bi-2212. Applied Surface Science, 2009, 255, 5503-5506.	6.1	14
78	Synthesis, structural and optical characterization of ZnO crystals grown in the presence of silver. Thin Solid Films, 2012, 520, 4717-4721.	1.8	14
79	Development of a new thermoelectric Bi2Ca2Co1.7Ox+Ca3Co4O9 composite. Scripta Materialia, 2014, 80, 1-4.	5.2	14
80	Heat Dissipation Interfaces Based on Vertically Aligned Diamond/Graphite Nanoplatelets. ACS Applied Materials & Interfaces, 2015, 7, 24772-24777.	8.0	14
81	Structural and optical characterization of Gd_2SiO_5 crystalline fibres obtained by laser floating zone. Optical Materials Express, 2017, 7, 868.	3.0	14
82	Photocatalytic Activity of Laserâ€Processed ZnO Micro/Nanocrystals. Physica Status Solidi (A) Applications and Materials Science, 2018, 215, 1800155.	1.8	14
83	Millimeter-sized few-layer suspended graphene membranes. Applied Materials Today, 2020, 21, 100879.	4.3	14
84	Surface activation pre-treatments for NCD films grown by HFCVD. Vacuum, 2009, 83, 1228-1232.	3.5	13
85	Nano carbon hybrids from the simultaneous synthesis of CNT/NCD by MPCVD. Diamond and Related Materials, 2009, 18, 160-163.	3.9	13
86	Electrical assisted laser floating zone (EALFZ) growth of 2212-BSCCO superconducting fibres. Applied Surface Science, 2011, 257, 5283-5286.	6.1	13
87	Structural, optical and magnetic resonance properties of TiO2 fibres grown by laser floating zone technique. Applied Surface Science, 2012, 258, 9143-9147.	6.1	13
88	Magnetite/hematite core/shell fibres grown by laser floating zone method. Applied Surface Science, 2013, 278, 203-206.	6.1	13
89	Spectroscopic Analysis of Eu ³⁺ Implanted and Annealed GaN Layers and Nanowires. Journal of Physical Chemistry C, 2015, 119, 17954-17964.	3.1	13
90	Structural, optical, and electrical properties of SmNbO4. Journal of Applied Physics, 2016, 120, .	2.5	13

#	Article	IF	CITATIONS
91	Shifting Lu2SiO5 crystal to eutectic structure by laser floating zone. Journal of the European Ceramic Society, 2018, 38, 2059-2067.	5.7	13
92	Dual Transduction of H2O2 Detection Using ZnO/Laser-Induced Graphene Composites. Chemosensors, 2021, 9, 102.	3.6	13
93	Electrochemical and photoluminescence response of laser-induced graphene/electrodeposited ZnO composites. Scientific Reports, 2021, 11, 17154.	3.3	13
94	Adhesion and Wear Behaviour of NCD Coatings on Si ₃ N ₄ by Micro-Abrasion Tests. Journal of Nanoscience and Nanotechnology, 2009, 9, 3938-3943.	0.9	12
95	Redox stability and high-temperature electrical conductivity of magnesium- and aluminium-substituted magnetite. Journal of the European Ceramic Society, 2013, 33, 2751-2760.	5.7	12
96	Microprobe analysis, iono- and photo-luminescence of Mn2+ activated ZnGa2O4 fibres. Nuclear Instruments & Methods in Physics Research B, 2013, 306, 195-200.	1.4	12
97	Stiff Diamond/Buckypaper Carbon Hybrids. ACS Applied Materials & Interfaces, 2014, 6, 22649-22654.	8.0	12
98	Effects of transition metal additives on redox stability and high-temperature electrical conductivity of (Fe,Mg)3O4 spinels. Journal of the European Ceramic Society, 2014, 34, 2339-2350.	5.7	12
99	Crystallization of iron-containing Si–Al–Mg–O glasses under laser floating zone conditions. Journal of Alloys and Compounds, 2014, 611, 57-64.	5.5	12
100	ZnO Transducers for Photoluminescence-Based Biosensors: A Review. Chemosensors, 2022, 10, 39.	3.6	12
101	Critical current density improvement in BSCCO superconductors by application of an electric current during laser floating zone growth. Physica C: Superconductivity and Its Applications, 2007, 460-462, 1347-1348.	1.2	11
102	Pulling rate and current intensity competition in an electrically assisted laser floating zone. Superconductor Science and Technology, 2009, 22, 065016.	3.5	11
103	Red and infrared luminescence from tetragonal YSZ:Pr3+ single crystal fibres grown by LFZ. Optical Materials, 2011, 34, 27-29.	3.6	11
104	ZnO Nano/Microstructures Grown by Laser Assisted Flow Deposition. Journal of Nano Research, 2012, 18-19, 129-137.	0.8	11
105	NbO/Nb2O5 core–shells by thermal oxidation. Journal of the European Ceramic Society, 2013, 33, 3077-3083.	5.7	11
106	Role of high microwave power on growth and microstructure of thick nanocrystalline diamond films: A comparison with large grain polycrystalline diamond films. Journal of Crystal Growth, 2014, 389, 83-91.	1.5	11
107	Prospects and challenges of iron pyroelectrolysis in magnesium aluminosilicate melts near minimum liquidus temperature. Physical Chemistry Chemical Physics, 2015, 17, 9313-9325.	2.8	11
108	Iron incorporation into magnesium aluminosilicate glass network under fast laser floating zone processing. Ceramics International, 2016, 42, 2693-2698.	4.8	11

#	Article	IF	CITATIONS
109	(Lu _{0.3} Gd _{0.7}) ₂ SiO ₅ :Y ³⁺ single crystals grown by the laser floating zone method: structural and optical studies. CrystEngComm, 2018, 20, 7386-7394.	2.6	11
110	Insights into the photoluminescence properties of gel-like carbon quantum dots embedded in poly(methyl methacrylate) polymer. Materials Today Communications, 2019, 18, 32-38.	1.9	11
111	Laser floating zone growth of Yb, or Nd, doped (Lu _{0.3} Gd _{0.7}) ₂ SiO ₅ oxyorthosilicate single-crystal rods with efficient laser performance. Journal of Materials Chemistry C, 2020, 8, 2065-2073.	5.5	11
112	Laser Floating Zone Growth: Overview, Singular Materials, Broad Applications, and Future Perspectives. Crystals, 2021, 11, 38.	2.2	11
113	LFZ fibre texture modification induced by electrical polarization. Physica C: Superconductivity and Its Applications, 2004, 408-410, 915-916.	1.2	10
114	Structural and optical properties on thulium-doped LHPG-grown Ta2O5 fibres. Microelectronics Journal, 2009, 40, 309-312.	2.0	10
115	Lithium niobate bulk crystallization promoted by CO2 laser radiation. Applied Surface Science, 2012, 258, 9457-9460.	6.1	10
116	Unusual redox behaviour of the magnetite/hematite core–shell structures processed by the laser floating zone method. Dalton Transactions, 2018, 47, 5646-5651.	3.3	10
117	A new concept of ceramic consumable anode for iron pyroelectrolysis in magnesium aluminosilicate melts. Ceramics International, 2016, 42, 11070-11076.	4.8	9
118	Influence of laser structural patterning on the tribological performance of C-alloyed W-S coatings. Surface and Coatings Technology, 2020, 394, 125822.	4.8	9
119	Deposition of TiB2 onto X40 CrMoV 5-1-1 steel substrates by DC magnetron sputtering. Vacuum, 2007, 81, 1519-1523.	3.5	8
120	Nucleation of nanocrystalline diamond on masked/unmasked Si3N4 ceramics with different mechanical pretreatments. Diamond and Related Materials, 2008, 17, 440-445.	3.9	8
121	Towards the understanding of the intentionally induced yellow luminescence in GaN nanowires. Physica Status Solidi C: Current Topics in Solid State Physics, 2013, 10, 667-672.	0.8	8
122	Spectroscopic studies of Tm-doped zirconia nanoparticles. Physica Status Solidi (B): Basic Research, 2013, 250, 815-820.	1.5	8
123	Millimeter sized graphene domains through in situ oxidation/reduction treatment of the copper substrate. Carbon, 2020, 169, 403-415.	10.3	8
124	Laser-Induced Hematite/Magnetite Phase Transformation. Journal of Electronic Materials, 2020, 49, 7187-7193.	2.2	8
125	On the half unit cell intergrowth of Bi2Sr2Ca3Cu4O12 with other superconducting phases in two-step annealed LFZ fibres. Physica C: Superconductivity and Its Applications, 2003, 398, 31-36.	1.2	7
126	Trapping control of phase development in zone melting of BiÂSrÂCaÂCuÂO superconducting fibres. Superconductor Science and Technology, 2003, 16, 392-397.	3.5	7

#	Article	IF	CITATIONS
127	NCD by HFCVD on a Si3N4-bioglass composite for biomechanical applications. Surface and Coatings Technology, 2006, 200, 6409-6413.	4.8	7
128	Effect of Eu2O3 doping on Ta2O5 crystal growth by the laser-heated pedestal technique. Journal of Crystal Growth, 2010, 313, 62-67.	1.5	7
129	Characterisation of interface formed at 650°C between AISI H13 steel and Al–12Si–1Cu aluminium melt. International Journal of Cast Metals Research, 2010, 23, 231-239.	1.0	7
130	New environmentally friendly Ba-Fe-O thermoelectric material by flexible laser floating zone processing. Scripta Materialia, 2018, 145, 54-57.	5.2	7
131	Effect of intergranular phase of Si3N4 substrates on MPCVD diamond deposition. Surface and Coatings Technology, 2002, 151-152, 521-525.	4.8	6
132	The effect of current direction on superconducting properties of BSCCO fibres grown by an electrically assisted laser floating zone process. Superconductor Science and Technology, 2006, 19, 15-21.	3.5	6
133	Bi–Sr–Ca–Cu–O superconducting fibres processed by the laser floating zone technique under different electrical current intensities. Superconductor Science and Technology, 2006, 19, 373-380.	3.5	6
134	Electric field-modified segregation in crystal fibers of colossal magnetoresistive La0.7Ca0.3MnO3. Journal of Crystal Growth, 2008, 310, 3568-3572.	1.5	6
135	Microwave dielectric permittivity and photoluminescence of Eu2O3 doped laser heated pedestal growth Ta2O5 fibers. Applied Physics Letters, 2008, 92, 252904.	3.3	6
136	Selfâ€Assembled Functionalized Graphene Nanoribbons from Carbon Nanotubes. ChemistryOpen, 2015, 4, 115-119.	1.9	6
137	Processing Effects on Properties of (Fe,Mg,Al) ₃ O ₄ Spinels as Potential Consumable Anodes for Pyroelectrolysis. Journal of the American Ceramic Society, 2016, 99, 1889-1893.	3.8	6
138	Guidelines to design multicomponent ferrospinels for high-temperature applications. RSC Advances, 2016, 6, 32540-32548.	3.6	6
139	Multiferroic interfaces in bismuth ferrite composite fibers grown by laser floating zone technique. Materials and Design, 2016, 90, 829-833.	7.0	6
140	Effect of laser irradiation on lithium niobate powders. Ceramics International, 2017, 43, 2504-2510.	4.8	6
141	Crystallization process, phase chemistry and transport properties of superconducting fibers prepared by the LFZ method followed by isothermal annealing. Physica C: Superconductivity and Its Applications, 1994, 235-240, 513-514.	1.2	5
142	Annealing time effect on Bi-2223 phase development in LFZ and EALFZ grown superconducting fibres. Applied Surface Science, 2006, 252, 4957-4963.	6.1	5
143	Room temperature PL characterization of micro and nanocrystalline diamond grown by MPCVD from Ar/H2/CH4 mixtures. Vacuum, 2007, 81, 1416-1420.	3.5	5
144	Structure and morphology of TiB2 duplex coatings deposited over X40 CrMoV 5-1-1 steel by DC magnetron sputtering. Vacuum, 2009, 83, 1291-1294.	3.5	5

#	Article	IF	CITATIONS
145	Electrical Polarization Effect on Bi2Ca2Co1.7Ox thermoelectrics grown by laser floating zone. Microscopy and Microanalysis, 2012, 18, 93-94.	0.4	5
146	Exotic Manganese Dioxide Structures in Niobium Oxides Capacitors. Microscopy and Microanalysis, 2012, 18, 99-100.	0.4	5
147	Ionic conductivity of directionally solidified zirconia–mullite eutectics. Solid State Ionics, 2014, 256, 45-51.	2.7	5
148	Correction to "Spectroscopic Analysis of Eu ³⁺ Implanted and Annealed GaN Layers and Nanowiresâ€: Journal of Physical Chemistry C, 2016, 120, 6907-6908.	3.1	5
149	Label-Free Nanoscale ZnO Tetrapod-Based Transducers for Tetracycline Detection. ACS Applied Nano Materials, 2022, 5, 1232-1243.	5.0	5
150	Preparation of superconductors of the BiSrCaCuO system by glass crystallization. Journal of the Less Common Metals, 1989, 150, 305-310.	0.8	4
151	Hard a-C/DLC coatings on Si3N4–bioglass composites. Diamond and Related Materials, 2006, 15, 944-947.	3.9	4
152	Directional solidification of ZrO2–BaZrO3 composites with mixed protonic–oxide ionic conductivity. Solid State Ionics, 2014, 262, 654-658.	2.7	4
153	Pressure effects on the dissipative behavior of nanocrystalline diamond microelectromechanical resonators. Journal of Micromechanics and Microengineering, 2015, 25, 025019.	2.6	4
154	High Thermoelectric Performances in Co-oxides Processed by a Laser Floating Zone Technique. Materials Today: Proceedings, 2015, 2, 654-660.	1.8	4
155	Improvement of thermoelectric properties of Ca0.9Gd0.1MnO3 by powder engineering through K2CO3 additions. Journal of Materials Science, 2019, 54, 3252-3261.	3.7	4
156	Relevance of the Spectral Analysis Method of Tilted Fiber Bragg Grating-Based Biosensors: A Case-Study for Heart Failure Monitoring. Sensors, 2022, 22, 2141.	3.8	4
157	Growth of the Bi-2223 phase after a short nucleation stage at high temperature. Physica B: Condensed Matter, 2001, 294-295, 700-704.	2.7	3
158	Enhancement of Bi-2223 phase formation by electrical assisted laser floating zone technique. Journal of Physics and Chemistry of Solids, 2006, 67, 416-418.	4.0	3
159	Structural and redox effects in iron-doped magnesium aluminosilicates. Journal of Crystal Growth, 2017, 457, 19-23.	1.5	3
160	Laser Floating Zone: General Overview Focusing on the Oxyorthosilicates Growth. , 2020, , .		3
161	Laser Melting Processing of ZrO ₂ –BaZrO ₃ Ceramic Eutectics. Science of Advanced Materials, 2013, 5, 1847-1856.	0.7	3
162	Optical Studies in Red/NIR Persistent Luminescent Cr-Doped Zinc Gallogermanate (ZGGO:Cr). Applied Sciences (Switzerland), 2022, 12, 2104.	2.5	3

#	Article	IF	CITATIONS
163	Bi-Ca-Sr-Cu-O superconductors obtained by glass crystallisation; Effect of potassium doping. Physica C: Superconductivity and Its Applications, 1989, 159, 273-276.	1.2	2
164	Abrasive Resistance of CVD Diamond Brazed Thick Films in Machining of WC Pre-Sintered Forms. Key Engineering Materials, 2002, 230-232, 193-198.	0.4	2
165	Acoustic emission detection of macro-indentation cracking of diamond coated silicon. Diamond and Related Materials, 2003, 12, 1744-1749.	3.9	2
166	Laser Assisted Flow Deposition: a New Method to Grow ZnO. Microscopy and Microanalysis, 2012, 18, 87-88.	0.4	2
167	The influence of photon excitation and proton irradiation on the luminescence properties of yttria stabilized zirconia doped with praseodymium ions. Nuclear Instruments & Methods in Physics Research B, 2013, 306, 207-211.	1.4	2
168	Prospects on laser processed wide band gap oxides optical materials. Proceedings of SPIE, 2013, , .	0.8	2
169	Defect luminescence in oxides nanocrystals grown by laser assisted techniques. , 2015, , .		2
170	Exploring the effects of silica and zirconia additives on electrical and redox properties of ferrospinels. Journal of the European Ceramic Society, 2017, 37, 2621-2628.	5.7	2
171	Intense red emission on dilute Mn-doped CaYAlO4-based ceramics obtained by laser floating zone. Journal of Materials Science: Materials in Electronics, 2019, 30, 21454-21464.	2.2	2
172	Directly MPCVD diamond-coated Si3N4 disks for dental applications. Diamond and Related Materials, 2005, 14, 626-630.	3.9	1
173	Reciprocating sliding behaviour of self-mated amorphous diamond-like carbon coatings on Si3N4 ceramics under tribological stress. Thin Solid Films, 2006, 515, 2192-2196.	1.8	1
174	The Effect of Annealing Temperature on the Transport Properties of BSCCO Fibres Grown by LFZ and EALFZ. Materials Science Forum, 2006, 514-516, 338-342.	0.3	1
175	From Micro to Nanometric Grain Size CVD Diamond Tools. Materials Research Society Symposia Proceedings, 2009, 1243, 1.	0.1	1
176	ZnO micro/nanocrystals grown by laser assisted flow deposition. , 2014, , .		1
177	Si ₃ N ₄ recubierto con diamante CVD mediante filamento caliente y plasma generado por microondas. Boletin De La Sociedad Espanola De Ceramica Y Vidrio, 2004, 43, 473-476.	1.9	1
178	On the Half Unit Cell Intergrowth of Bi2Sr2Ca3Cu4Ox with Other Superconducting Phases in Two-step Annealed LFZ Fibers. Microscopy and Microanalysis, 2002, 8, 1352-1353.	0.4	0
179	Cutting of Free Standing CVD Diamond Films by Optical Fibre Guided Nd:YAG Laser. Materials Science Forum, 2004, 455-456, 614-618.	0.3	0
180	Vortex dimensionality and pinning efficiency in granular specimens having a narrow weak-link critical current distribution. Journal of Physics: Conference Series, 2006, 43, 618-622.	0.4	0

#	Article	IF	CITATIONS
181	Preparation and Properties of New Superconductor Material MgB ₂ . Materials Science Forum, 2006, 514-516, 333-337.	0.3	0
182	Ionic conductivity of eutectic mullite-zirconia fibres. , 2012, , .		0
183	Quantification of Microstructural Features in Carbon Nanotube/Nanodiamond Hybrids. Microscopy and Microanalysis, 2012, 18, 85-86.	0.4	0
184	ZnGa2O4:Mn2+ Phosphors Grown by Laser Floating Zone. Microscopy and Microanalysis, 2012, 18, 105-106.	0.4	0
185	Microstructure of Mullite-zirconia Fibres Grown by Directional Solidification. Microscopy and Microanalysis, 2012, 18, 103-104.	0.4	0
186	Dielectric properties and microstructure of CaCu <inf>3</inf> Ti <inf>4−x</inf> Mn <inf>x</inf> O <inf>12</inf> fibres grown by laser floating zone technique. , 2012, , .		0
187	Dielectric characterization of low-loss calcium strontium titanate fibers produced by laser floating zone technique for wireless communication. Physica Status Solidi (A) Applications and Materials Science, 2014, 211, 2086-2089.	1.8	0
188	Nd:YAG laser scribed zinc oxide on semi-flexible copper foils. Materials Letters: X, 2020, 5, 100038.	0.7	0
189	Simultaneous CVD Growth of Nanostructured Carbon Hybrids. NATO Science for Peace and Security Series A: Chemistry and Biology, 2015, , 111-117.	0.5	0